

Unified quark-hadron EoS and CEP in the QCD phase diagram ¹

David Blaschke

Institute of Theoretical Physics, University Wrocław, Poland
Bogoliubov Laboratory for Theoretical Physics, JINR Dubna, Russia

Workshop on Criticality in QCD and the Hadron Resonance Gas
Wrocław, 31. July 2020

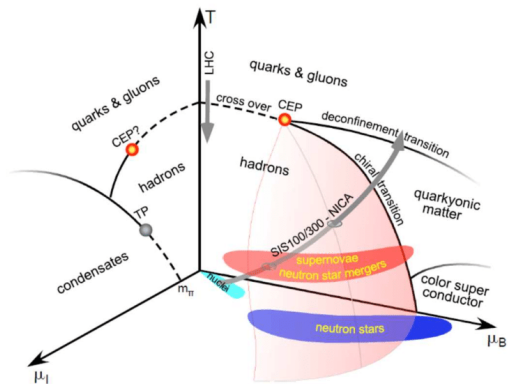


¹Collab: N.-U. Bastian, K. Devyatyarov, A. Dubinin, A. Friesen, G. Röpke, ...

Plan of the talk

- 1 Motivation: 3D phase diagram and astrophysics of deconfinement in supernovae, mergers and neutron stars
- 2 How to construct a unified approach ?
 - Cluster decomposition: quarks, gluons, mesons, baryons → Beth-Uhlenbeck approach
 - Two challenges:
 - a) confinement of quarks and gluons and
 - b) Mott dissociation of hadrons
 - Backreaction via order parameters:
→ Polyakov-loop and chiral condensate (quark masses)
- 3 A simple model for quark-nuclear matter at low temperatures
→ phase diagram: CEP and crossover
- 4 Cluster decomposition for quark-gluon matter with Mott-HRG
→ comparison to lattice QCD

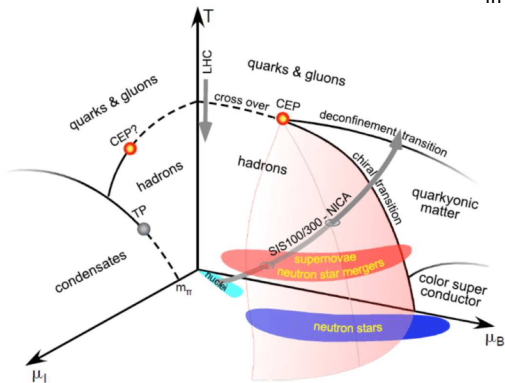
QCD Phase Diagram: Astrophysics vs. Heavy-Ion Coll.



From: NuPECC Long Range Plan 2017

QCD Phase Diagram: Astrophysics vs. Heavy-Ion Coll.

Prominent contributions to deconfinement in modern multimessenger Astrophysics:



- Quark deconfinement transition triggers the **supernova explosion** of a very massive ($M = 50M_{\odot}$) blue supergiant progenitor star
T. Fischer et al., Nature Astron. 2 (2018) 960
- Unambiguous signal of a strong phase transition in the postmerger GW from a binary **NS merger** predicted
A. Bauswein et al., Phys. Rev. Lett. 122 (2019) 061102
- Strong deconfinement phase transition in NS can be detected by observing the **mass twin star** phenomenon
D. B. et al., Universe 6 (2020) 81

From: NuPECC Long Range Plan 2017

Φ —Derivable Approach to the Cluster Virial Expansion

$$\Omega = \sum_{l=1}^A \Omega_l = \sum_{l=1}^A \left\{ c_l [\text{Tr} \ln (-G_l^{-1}) + \text{Tr} (\Sigma_l G_l)] + \sum_{\substack{i,j \\ i+j=l}} \Phi[G_i, G_j, G_{i+j}] \right\},$$

$$G_A^{-1} = G_A^{(0)-1} - \Sigma_A, \quad \Sigma_A(1 \dots A, 1' \dots A', z_A) = \frac{\delta \Phi}{\delta G_A(1 \dots A, 1' \dots A', z_A)}$$

Stationarity of the thermodynamical potential is implied

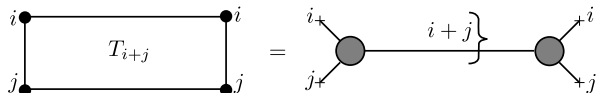
$$\frac{\delta \Omega}{\delta G_A(1 \dots A, 1' \dots A', z_A)} = 0.$$

Cluster virial expansion follows for this Φ – functional



Figure: The Φ functional for A –particle correlations with bipartitions $A = i + j$.

Green's function and T-matrix: separable approximation



The T_A matrix fulfills the Bethe-Salpeter equation in ladder approximation

$$T_{i+j}(1, 2, \dots, A; 1', 2', \dots, A'; z) = V_{i+j} + V_{i+j} G_{i+j}^{(0)} T_{i+j},$$

which in the separable approximation for the interaction potential,

$$V_{i+j} = \Gamma_{i+j}(1, 2, \dots, i; i+1, i+2, \dots, i+j) \Gamma_{i+j}(1', 2', \dots, i'; (i+1)', (i+2)', \dots, (i+j)'),$$

leads to the closed expression for the T_A matrix

$$T_{i+j}(1, 2, \dots, i+j; 1', 2', \dots, (i+j)'; z) = V_{i+j} \{1 - \Pi_{i+j}\}^{-1},$$

with the generalized polarization function

$$\Pi_{i+j} = \text{Tr} \left\{ \Gamma_{i+j} G_i^{(0)} \Gamma_{i+j} G_j^{(0)} \right\}$$

The one-frequency free i -particle Green's function is defined by the $(i-1)$ -fold Matsubara sum

$$\begin{aligned} G_i^{(0)}(1, 2, \dots, i; \Omega_i) &= \sum_{\omega_1 \dots \omega_{i-1}} \frac{1}{\omega_1 - E(1)} \frac{1}{\omega_2 - E(2)} \cdots \frac{1}{\Omega_i - (\omega_1 + \dots + \omega_{i-1}) - E(i)} \\ &= \frac{(1-f_1)(1-f_2) \dots (1-f_i) - (-)^i f_1 f_2 \dots f_i}{\Omega_i - E(1) - E(2) - \dots - E(i)}. \end{aligned}$$

Useful relationships for many-particle functions

$$G_{i+j}^{(0)} = G_{i+j}^{(0)}(1, 2, \dots, i+j; \Omega_{i+j}) = \sum_{\Omega_i} G_i^{(0)}(1, 2, \dots, i; \Omega_i) G_j^{(0)}(i+1, i+2, \dots, i+j; \Omega_j) .$$

Another set of useful relationships follows from the fact that in the ladder approximation both, the full two-cluster ($i+j$ particle) T matrix and the corresponding Greens' function

$$G_{i+j} = G_{i+j}^{(0)} \{1 - \Pi_{i+j}\}^{-1} \quad (1)$$

have similar analytic properties determined by the $i+j$ cluster polarization loop integral and are related by the identity

$$T_{i+j} G_{i+j}^{(0)} = V_{i+j} G_{i+j} . \quad (2)$$

which is straightforwardly proven by multiplying Equation for the T_{i+j} - matrix with $G_{i+j}^{(0)}$ and using Equation (1). Since these two equivalent expressions in Equation (2) are at the same time equivalent to the two-cluster irreducible Φ functional these functional relations follow

$$\begin{aligned} T_{i+j} &= \delta\Phi / \delta G_{i+j}^{(0)} , \\ V_{i+j} &= \delta\Phi / \delta G_{i+j} . \end{aligned}$$

Next we prove the relationship to the Generalized Beth-Uhlenbeck approach!

GBU EoS from the Φ -derivable approach

Consider the partial density of the A -particle state defined as

$$n_A(T, \mu) = -\frac{\partial \Omega_A}{\partial \mu} = -\frac{\partial}{\partial \mu} d_A \int \frac{d^3 q}{(2\pi)^3} \int \frac{d\omega}{2\pi} \left[\ln(-G_A^{-1}) + \text{Tr}(\Sigma_A G_A) \right] + \sum_{i+j=A} \Phi[G_i, G_j, G_{i+j}]. \quad (3)$$

Using spectral representation for $F(\omega)$ and Matsubara summation

$$F(i z_n) = \int_{-\infty}^{\infty} \frac{d\omega}{2\pi} \frac{\text{Im} F(\omega)}{\omega - i z_n}, \quad \sum_{z_n} \frac{c_A}{\omega - i z_n} = f_A(\omega) = \frac{1}{\exp[(\omega - \mu)/T] - (-1)^A}$$

with the relation $\partial f_A(\omega)/\partial \mu = -\partial f_A(\omega)/\partial \omega$ we get for Equation (3) now

$$n_A(T, \mu) = -d_A \int \frac{d^3 q}{(2\pi)^3} \int \frac{d\omega}{2\pi} f_A(\omega) \frac{\partial}{\partial \omega} \left[\text{Im} \ln(-G_A^{-1}) + \text{Im}(\Sigma_A G_A) \right] + \sum_{i+j=A} \frac{\partial \Phi[G_i, G_j, G_A]}{\partial \mu},$$

where a partial integration over ω has been performed For two-loop diagrams of the sunset type holds a cancellation² which we generalize here for cluster states

$$d_A \int \frac{d^3 q}{(2\pi)^3} \int \frac{d\omega}{2\pi} f_A(\omega) \frac{\partial}{\partial \omega} (\text{Re} \Sigma_A \text{Im} G_A) - \sum_{i+j=A} \frac{\partial \Phi[G_i, G_j, G_A]}{\partial \mu} = 0.$$

Using generalized optical theorems we can show that ($G_A = |G_A| \exp(i\delta_A)$)

$$\frac{\partial}{\partial \omega} \left[\text{Im} \ln(-G_A^{-1}) + \text{Im} \Sigma_A \text{Re} G_A \right] = 2 \text{Im} \left[G_A \text{Im} \Sigma_A \frac{\partial}{\partial \omega} G_A^* \text{Im} \Sigma_A \right] = -2 \sin^2 \delta_A \frac{\partial \delta_A}{\partial \omega}.$$

The density in the form of a generalized Beth-Uhlenbeck EoS follows

$$n(T, \mu) = \sum_{i=1}^A n_i(T, \mu) = \sum_{i=1}^A d_i \int \frac{d^3 q}{(2\pi)^3} \int \frac{d\omega}{2\pi} f_i(\omega) 2 \sin^2 \delta_i \frac{\partial \delta_i}{\partial \omega}.$$

²B. Vanderheyden & G. Baym, J. Stat. Phys. (1998), J.-P. Blaizot et al., PRD (2001)

Example: Mott Dissociation of Pions in Quark Matter

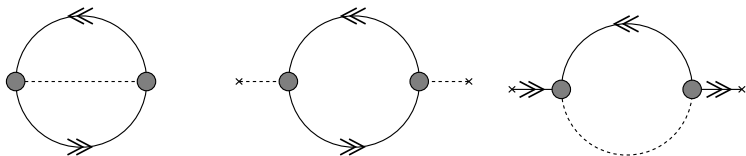


Figure: The Φ functional (left panel) for the case of mesons in quark matter, where the bosonic meson propagator is defined by the dashed line and the fermionic quark propagators are shown by the solid lines with arrows. The corresponding meson and quark selfenergies are shown in the middle and right panels, respectively.

Mott Dissociation of Pions in Quark Matter

The meson polarization loop $\Pi_M(q, z)$ enters the definition of the meson T matrix

$$T_M^{-1}(q, \omega + i\eta) = G_S^{-1} - \Pi_M(q, \omega + i\eta) = |T_M(q, \omega)|^{-1} e^{-i\delta_M(q, \omega)},$$

which in the polar representation introduces a phase shift $\delta_M(q, \omega) = \arctan(\Im T_M / \Re T_M)$, that results in a generalized Beth-Uhlenbeck equation of state for the thermodynamics of the consistently coupled quark-meson system

$$\Omega = \Omega_{\text{MF}} + \Omega_M,$$

where the selfconsistent quark meanfield contribution is

$$\Omega_{\text{MF}} = \frac{\sigma_{\text{MF}}^2}{4G_S} - 2N_c N_f \int \frac{d^3 p}{(2\pi)^3} \left[E_p + T \ln \left(1 + e^{-(E_p - \Sigma_+ - \mu)/T} \right) + T \ln \left(1 + e^{-(E_p + \Sigma_- + \mu)/T} \right) \right],$$

The mesonic contribution to the thermodynamics is

$$\Omega_M = d_M \int \frac{d^3 k}{(2\pi)^3} \int \frac{d\omega}{2\pi} \left\{ \omega + 2T \ln \left[1 - e^{-\omega/T} \right] \right\} 2 \sin^2 \delta_M(k, \omega) \frac{\delta_M(k, \omega)}{d\omega},$$

Mott Dissociation of Pions in Quark Matter

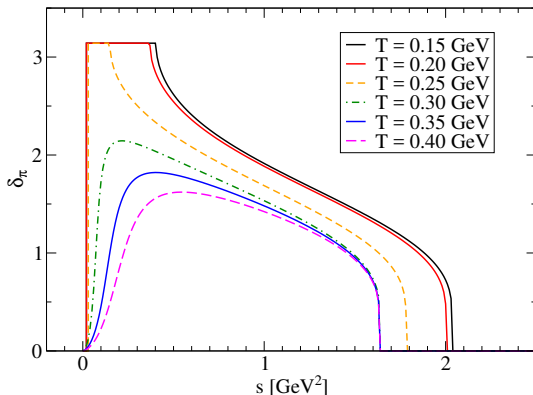


Figure: Phase shift of the pion as a quark-antiquark state for different temperatures, below and above the Mott dissociation temperature.

From D.B., M. Buballa, et al., *Ann. Phys.* 348 (2014) 228.

See also D.B., A. Dubinin, D. Ebert, A.V. Friesen, *PPN Lett.* 15 (2018) 230.

Φ -derivable cluster expansion for quark-nuclear matter

Cluster decomposition of the thermodynamic potential

$$\begin{aligned}\Omega &= \sum_i \Omega_i \\ &= \sum_i \left\{ c_i [\text{Tr} \ln (-G_i^{-1}) + \text{Tr} (\Sigma_i G_i)] + \sum_{\substack{j,k \\ j+k=i}} \Phi[G_j, G_k, G_{j+k}] \right\},\end{aligned}$$

generates the partial densities

$$\begin{aligned}n_j(T, \mu) &= -\frac{\partial \Omega}{\partial \mu_j} = \sum_{i=1} A_{ij} n_i(T, \mu) \\ &= \sum_{i=1} A_{ij} g_i \int \frac{d^3 p}{(2\pi)^3} \int \frac{dE}{2\pi} f_i(E) 2 \sin^2 \delta_i(E) \frac{d\delta_i(E)}{dE},\end{aligned}$$

Based on: N.-U. F. Bastian and D.B., arXiv:1812.11889

Φ -derivable cluster expansion for quark-nuclear matter

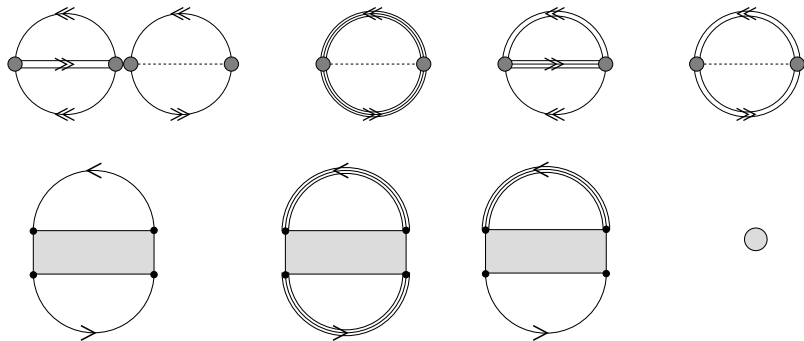


Figure:

Upper row: full set of sunset type diagrams.

Lower row: after collapsing the diquark and meson-propagators (\rightarrow mean fields).

Relativistic Density Functional Approach to Nuclear Matter

In case of color confinement all closed loop diagrams with Q- and D-lines vanish. The system reduces to the M-B- system. The Φ -functional becomes a density functional.

$$\Phi = \text{Diagram} \Rightarrow \mathcal{U} = \text{Diagram}$$

The diagram on the left is a circle with two vertices (grey dots) on a horizontal dashed line. The top and bottom arcs of the circle have arrows pointing clockwise. The diagram on the right is a square with a grey shaded center labeled G_{i+j} . The top and bottom edges of the square have curly braces labeled $\{i\}$ and $\{j\}$ respectively, pointing outwards.

$$\Omega = T \sum_{i=n,p,\Lambda,\dots} c_i \left[\text{Tr} \ln S_{i,qu}^{-1} + \sum_{j=S,V} n_{i,j} \Sigma_{i,j} \right] + U \{ [n_{i,S}, n_{i,V}] \} ,$$

$$\frac{\partial \Omega}{\partial n_{i,S}} = \frac{\partial \Omega}{\partial n_{i,V}} = 0, \quad i = n, p, \Lambda, \dots,$$

$$\frac{\partial U}{\partial n_{i,S}} = \Sigma_{i,S}, \quad \frac{\partial U}{\partial n_{i,V}} = \Sigma_{i,V} .$$

The baryon quasiparticle propagators fulfill the Dyson equations $S_{i,qu}^{-1} = S_{i,0}^{-1} - \Sigma_{i,S} - \Sigma_{i,V}$,

$$\text{Diagram} = \text{Diagram} + \text{Diagram}$$

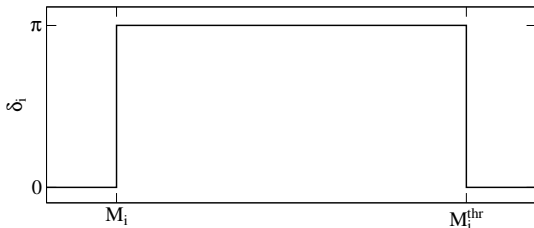
The diagram on the left is a horizontal line with a curly brace labeled $\{i\}$ above it and "qu" below it. The diagram in the middle is a horizontal line with a curly brace labeled $\{i\}$ above it and "id" below it. The diagram on the right is a horizontal line with a curly brace labeled $\{i\}$ above it and "id" below it on the left, and a curly brace labeled $\{i\}$ above it and "qu" below it on the right. A square with a grey shaded center labeled G_{i+j} is attached to the line between the two curly braces. The top and bottom edges of the square have curly braces labeled $\{j\}$ and "qu" above them, pointing outwards.

Φ -derivable cluster expansion for quark-nuclear matter

$$n_i^{\text{free}} = g_i \int \frac{d^3 p}{(2\pi)^3} \int \frac{dM}{2\pi} f_i \left(\sqrt{p^2 + M^2} + V_i \right) 2 \sin^2 \delta_i(M) \frac{d\delta_i(M)}{dM}$$

Phase shift model:

$\delta_{i=p,n}(M) = \pi \Theta(M - M_i) \Theta(M_i^{\text{thr}} - M)$ with $M_p^{\text{thr}} = 2M_u + M_d$ etc.



$$\begin{aligned} n_{i=p,n} &= g_i \int \frac{d^3 p}{(2\pi)^3} \left[f_i(\sqrt{p^2 + M_i^2} + V_i) - f_i(\sqrt{p^2 + (M_i^{\text{thr}})^2} + V_i) \right] \Theta(M_i^{\text{thr}} - M) \\ &= \left(n_N^{\text{qu}} - n_N^{\text{thr}} \right) \Theta(M_i^{\text{thr}} - M) \end{aligned}$$

Selfenergies: Relativistic Density Functionals

Quark Matter: $U_{\text{SFM}} = D(n_v)n_{q,s}^{2/3} + an_{q,v}^2$.

$$S_{\text{SFM}} = \frac{2}{3}D(n_{q,v})n_{q,s}^{-1/3}, \quad D(n_v) = D_0 \exp(-\alpha n_{q,v}^2) \quad (5)$$

Nuclear Matter:

$$U_{\text{DD2}} = -\frac{1}{2} \frac{\Gamma_\sigma^2}{m_\sigma^2} n_s^2 + \frac{1}{2} \frac{\Gamma_\omega^2}{m_\omega^2} n_v^2 + \frac{1}{2} \frac{\Gamma_\rho^2}{m_\rho^2} n_{vi}^2, \quad (6)$$

Scalar self-energy: $S_{\text{DD2}} = -(\Gamma_\sigma^2/m_\sigma^2)n_s$, Vector self-energy:

$$V_{\text{DD2},i} = \frac{\Gamma_\omega^2}{m_\omega^2} n_v + \tau_i \frac{\Gamma_\rho^2}{m_\rho^2} n_{vi} - \frac{\Gamma_\sigma \Gamma'_\sigma}{m_\sigma^2} n_s^2 + \frac{\Gamma_\omega \Gamma'_\omega}{m_\omega^2} n_v^2 + \frac{\Gamma_\rho \Gamma'_\rho}{m_\rho^2} n_{vi}^2. \quad (7)$$

Thermodynamics of quark-nuclear matter

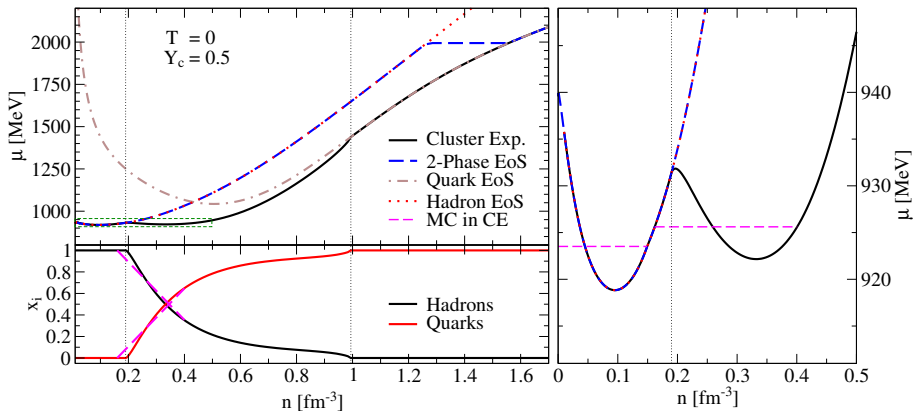
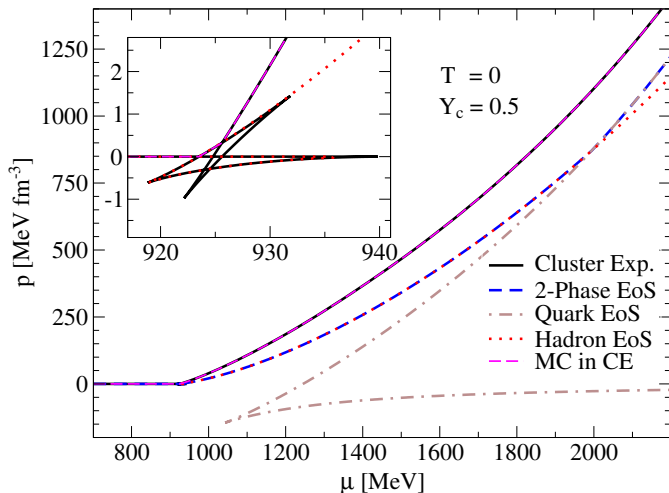


Figure: Van der Waals type thermodynamic behaviour with two first order phase transitions: liquid-gas and deconfinement. Note the wide density range for quark-hadron mixture after the deconfinement transition.

Maxwell construction for quark-nuclear matter EoS



Phase diagram of quark-nuclear matter

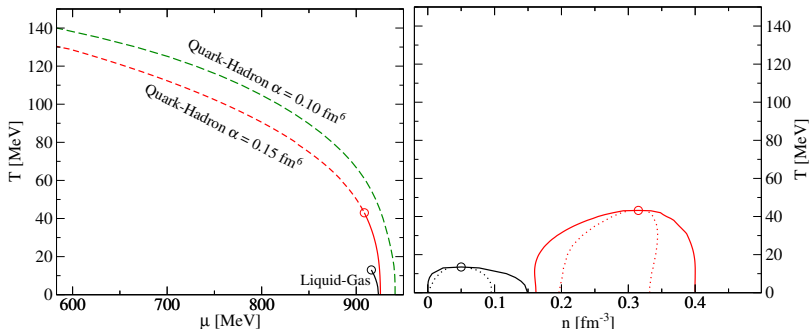


Figure: Phase diagram of the cluster expansion, with the liquid-gas phase transition (black) and two parametrizations of quark-hadron transition. One features a first order phase transition (red) with mixed phase and a critical endpoint at $T_C = 43 \text{ MeV}$ and $\mu_C = 909 \text{ MeV}$. The other represents a crossover all over scenario (green) without critical endpoint. Right panel: the borders of the phase coexistence regions (binodals) for liquid-gas (black) and quark-hadron (red) transitions; dotted lines show the spinodal region of thermodynamic instability ($\partial\mu/\partial n < 0$).

More details in: N.-U. F. Bastian and D.B., arXiv:1812.11889

Unified q-g-H EoS in the Beth-Uhlenbeck approach

$$P_{\text{total}}(T) = P_{\text{MHRG}}(T) + P_{\text{PNJL}}(T) + P_{\text{pert}}(T), \quad (8)$$

Beth-Uhlenbeck model for HRG with Mott dissociation

$$P_{\text{MHRG}}(T) = \sum_{i=M,B} P_i(T), \quad (9)$$

$$P_i(T) = \mp d_i \int_0^\infty \frac{dp p^2}{2\pi^2} \int_0^\infty \frac{dM}{\pi} T \ln \left(1 \mp e^{-\sqrt{p^2+M^2}/T} \right) \frac{d\delta_i(M^2; T)}{dM}$$

Simple phase shift model (see above), fulfilling Levinson's theorem

$$\delta_i(M^2; T) = \pi [\Theta(M - M_i) - \Theta(M - M_{\text{thr},i}(T))] \Theta(M_{\text{thr},i}(T) - M_i).$$

$$P_i(T) = \mp d_i \int_0^\infty \frac{dp p^2}{2\pi^2} T \ln \left(\frac{1 \mp e^{-\sqrt{p^2+M_i^2}/T}}{1 \mp e^{-\sqrt{p^2+M_{\text{thr},i}(T)}^2/T}} \right) \Theta(M_{\text{thr},i}(T) - M_i) \quad (10)$$

Model for the continuum threshold

$$M_{\text{thr},i}(T) = \sqrt{2} [(N_i - N_s)m_l(T) + N_s m_s(T)], \quad q = l, s$$

$$m_q(T) = \Delta m \Delta_{l,s}(T) + m_{q,0}, \quad m_{l,0} = 5 \text{ MeV}, \quad m_{s,0} = 135 \text{ MeV}$$

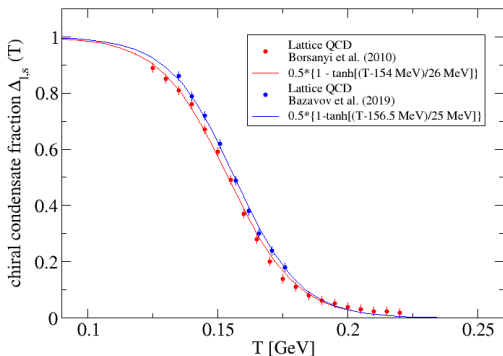


Figure: Chiral condensate fraction and fit function.

HRG with Mott dissociation

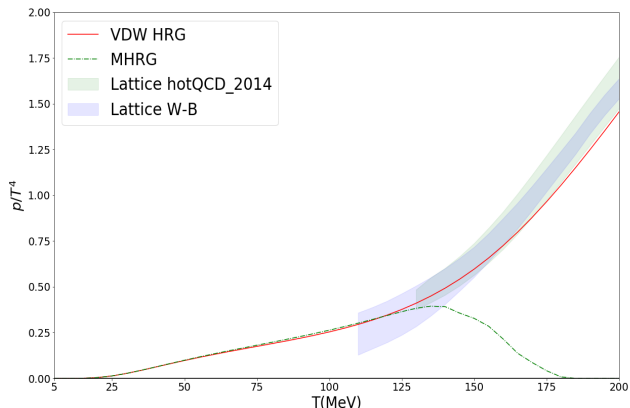


Figure: Hadron resonance gas model without and with Mott dissociation of hadrons, comparison with lattice QCD thermodynamics.

From K. Devyatyarov, Master Thesis, NRNU (MEPhI) Moscow (2020).

Polyakov-loop improved Nambu–Jona-Lasinio model

The underlying quark and gluon thermodynamics is divided into a perturbative contribution $P_{\text{pert}}(T)$ which is treated as virial correction in two-loop order and a nonperturbative part described within a PNJL model

$$P_{\text{PNJL}}(T) = P_Q(T) + U(\phi, T) \quad (11)$$

where the quark quasiparticle pressure contribution is

$$P_Q(T) = 4N_c \sum_{q=u,d,s} \int \frac{dp}{2\pi^2} \frac{p^2}{3} T \ln [1 + 3\phi(1 + Y)Y + Y^3], \quad Y = e^{-E(p)/T} \quad (12)$$

and $U(\phi; T)$ is the nonperturbative gluon background in a meanfield approximation using the polynomial fit of Ratti et al. PRD **73** (2006)

$$U(\phi, T) = \frac{b_2(T)}{2} \phi^2 + \frac{b_3}{3} \phi^3 - \frac{b_4}{4} \phi^4 \quad (13)$$

Perturbative contribution: two-loop diagram

The 2-loop contribution to the pressure (quark-gluon sunset diagram) in the massless limit is defined by

$$P_{pert}(\phi, T) = -\frac{8}{\pi}\alpha_s T^4 \left\{ I_\Lambda(\phi, T) + \frac{3}{\pi^2} [I_\Lambda(\phi, T)]^2 \right\} \quad (14)$$

with the integral


$$I_\Lambda(\phi, T) = \int_{\Lambda/T}^{\infty} dx \, x \, f_\phi(x), \quad (15)$$

where the Polyakov-loop generalized Fermi distribution function is

$$f_\phi(x) = [\phi(1 + 2Y)Y + Y^3]/[1 + 3\phi(1 + Y)Y + Y^3], \quad Y = \exp(-x) \quad (16)$$

and $\Lambda = m_l(T)$ is the momentum range below which nonperturbative physics dominates, accounted for by a dynamically generated quark mass. We use here a temperature dependent, regularized running coupling

$$\alpha_s = \frac{g^2}{4\pi} = \frac{12\pi}{11N_c - 2N_f} \left(\frac{1}{\ln(r^2/c^2)} - \frac{c^2}{r^2 - c^2} \right), \quad (17)$$

where $r = 3.2T$, $c = 350$ MeV and $N_c = N_f = 3$. 

Gap equation for the Polyakov loop

$$\frac{dP_{\text{total}}}{d\phi} = \frac{dU(\phi, T)}{d\phi} + \frac{dP_Q(T)}{d\phi} + \frac{dP_{\text{pert}}(T)}{d\phi} = 0$$

$$\frac{dU(\phi, T)}{d\phi} = b_2(T)\phi + b_3\phi^2 - b_4\phi^3$$

$$\frac{dP_Q(T)}{d\phi} = 4N_c \sum_{q=u,d,s} \int \frac{dp}{2\pi^2} \frac{p^2}{1 + 3\phi(1+Y)Y + Y^3} \frac{(1+Y)Y}{Y}, \quad Y = e^{-E(p)/T}$$

$$\frac{dP_{\text{pert}}(T)}{d\phi} = -\frac{8}{\pi} \alpha_s T^4 \left[\frac{dl(\phi, T)}{d\phi} + \frac{6}{\pi^2} l(\phi, T) \frac{dl(\phi, T)}{d\phi} \right]$$

$$\frac{dl(\phi, T)}{d\phi} = \int_{\Lambda/T}^{\infty} dx \times \frac{df_{\phi}(\omega)}{d\phi},$$

$$\frac{df_{\phi}(\omega)}{d\phi} = \frac{Y + 2Y^2 - 2Y^4 - Y^5}{(1 + 3\phi(1+Y)Y + Y^3)^2} = \frac{(1+2Y)Y - (2+Y)Y^4}{(1 + 3\phi(1+Y)Y + Y^3)^2}$$

Gap equation for the Polyakov loop

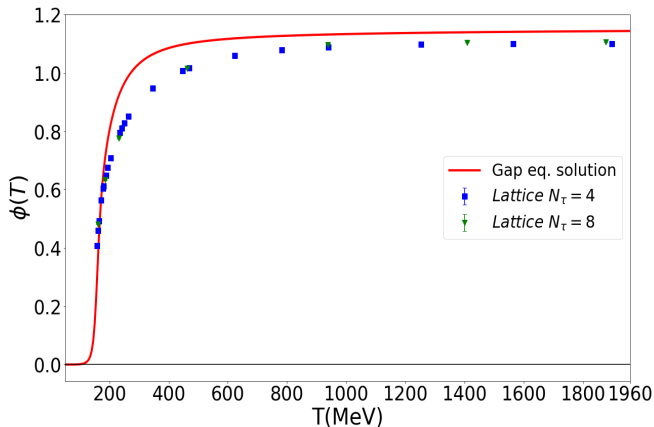


Figure: Temperature dependence of the Polyakov loop (PL) within the unified q-g-H model, comparison with renormalized PL of S. Gupta, K. Huebner and O. Kaczmarek, PRD 77 (2008).

From D.B., K. Devyatyarov and O. Kaczmarek, in preparation (2020).

Thermodynamics of the unified q-g-H model

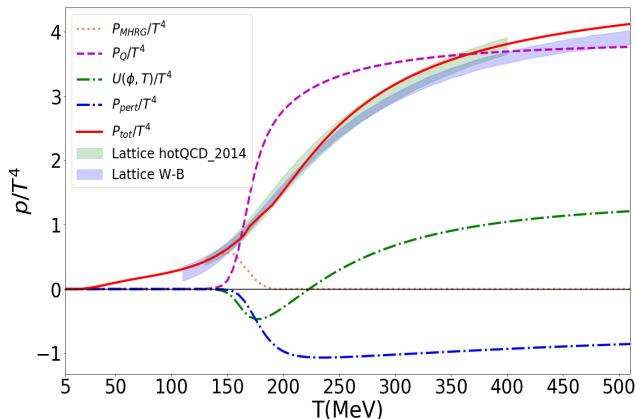


Figure: Temperature dependence of the total pressure and its components within the unified q-g-H model, comparison with lattice QCD data.

From D.B., K. Devyatyarov and O. Kaczmarek, in preparation (2020).

Compare with earlier results: D.B., A. Dubinin, L. Turko, APPB 10, 473 (2017).

Thermodynamics of the unified q-g-H model

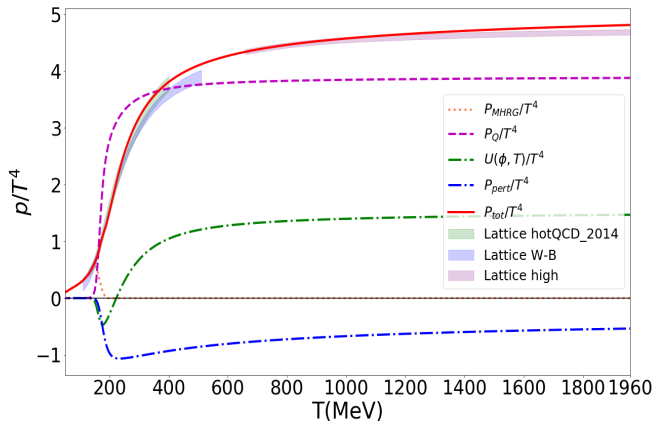


Figure: Temperature dependence of the total pressure and its components within the unified q-g-H model, comparison with lattice QCD data up to $T = 1960$ MeV. From D.B., K. Devyatyarov and O. Kaczmarek, in preparation (2020).

Consistency check: Chiral condensate and hadron fraction

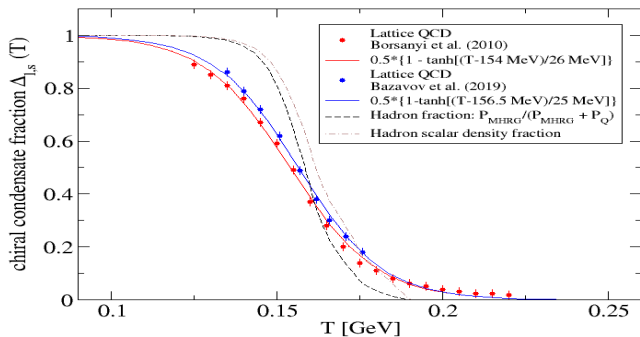


Figure: MHRG pressure fraction and scalar density fraction compared to lattice QCD data for the chiral condensate ratio.

From D.B., K. Devyatyarov and O. Kaczmarek, in preparation (2020).

"In-hadron condensate": Brodsky, Roberts, et al., Phys.Rev.C 85 (2012)

Consistency check: Chiral condensate and hadron fraction

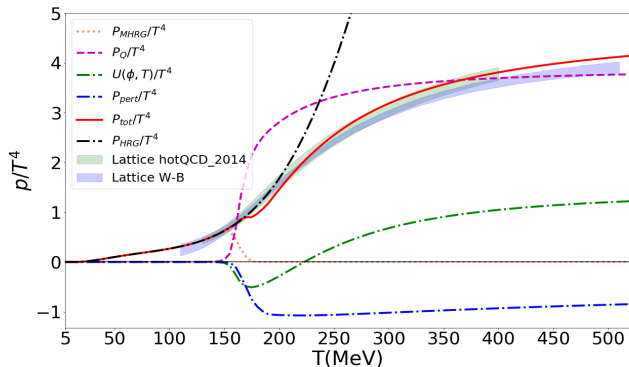


Figure: Temperature dependence of the total pressure and its components within the unified q-g-H model, comparison with lattice QCD data..

From D.B., K. Devyatyarov and O. Kaczmarek, in preparation (2020).

Ratios of susceptibilities - an example

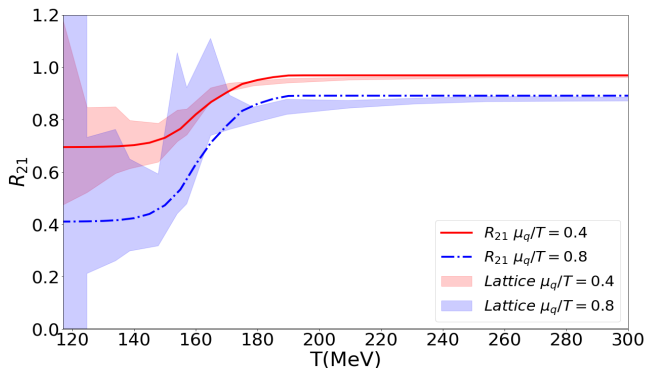


Figure: From D.B., K. Devyatyarov and O. Kaczmarek, in preparation (2020).

Summary

- equivalence of Φ -derivable and generalized Beth-Uhlenbeck approaches shown for Φ functionals that are two-loop diagrams
- cluster virial expansion developed for sunset-type Φ functionals made of cluster Green's functions and a cluster T-matrix
- selfconsistent density-functional approach to quark matter with confinement and chiral symmetry breaking obtained as limiting case
- low-T phase diagram obtained, Existence of CEP depends on details of the density functional
- finite-T thermodynamics of unified q-g-H model in agreement with lattice QCD data

Outlook

- improvement of phase shifts: continuum correlations and hadron broadening
- finite- μ extension straightforward, is there a CEP?
- RDF as confining mechanism at low temperatures - combination with Polyakov-loop?